

Reading Between the Fibres: AI Reveals Hidden Patterns in MASLD

M. K. Wojciechowska^{1,2*}, M. Thing^{3*}, Y. Hu^{1,2}, G. Mazzoni⁴, L. M. Harder⁴, M. P. Werge³, V. Das⁴, J. M. Martinez⁴, C. A. Prada-Medina⁵, M. Vyberg³, R. Goldin⁶, R. Serizawa⁷, E. D. Galsgaard⁴, D. J. Woodcock⁸, H. Hvid⁴, D. R. Pfister⁴, V. I. Jurtz^{4**}, L. L. Gluud^{3**}, J. Rittscher^{1,9**}

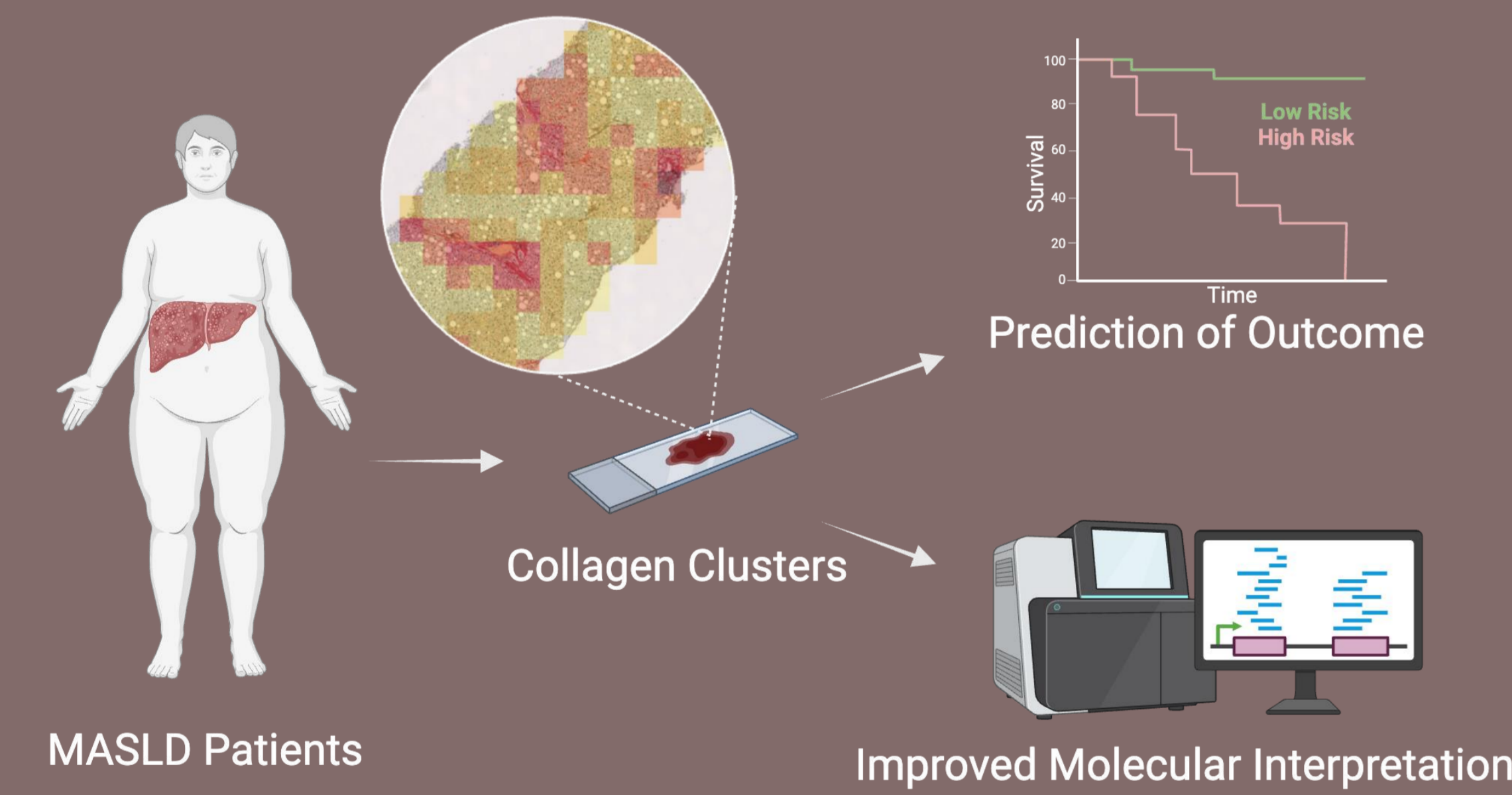
¹Big Data Institute, University of Oxford, United Kingdom; ²Nuffield Department of Medicine, University of Oxford, UK; ³Gastro Unit, Copenhagen University Hospital Hvidovre, Denmark; ⁴Novo Nordisk A/S, Copenhagen, Denmark; ⁵Novo Nordisk Research Center Oxford, Novo Nordisk A/S, Oxford, UK; ⁶Imperial College London, UK; ⁷Department of Pathology, Copenhagen University Hospital Hvidovre, Denmark; ⁸Nuffield Department of Surgical Sciences, University of Oxford, UK; ⁹Department of Engineering Science, University of Oxford, UK; * ** These authors contributed equally to this work.



Objectives

We set out to provide a more granular assessment of liver fibrosis – one which overcomes the limitations of collagen proportionate area (CPA) and traditional fibrosis scoring.

- To identify patterns of fibrosis that can predict liver-related events.
- To assess if local morphology of the extracellular matrix (ECM) can be associated with established transcriptomic markers of fibrogenesis.



Our methods were developed and validated on a group of 187 MASLD patients and 15 healthy volunteers from the FLINC cohort.

Conclusions

Collagen phenotypes bridge the gap between histology and transcriptomic profiling allowing for a cost-effective analysis of retrospective cohorts of patients with MASLD. This approach can be used to develop histology-based biomarkers for disease progression.

Contact us

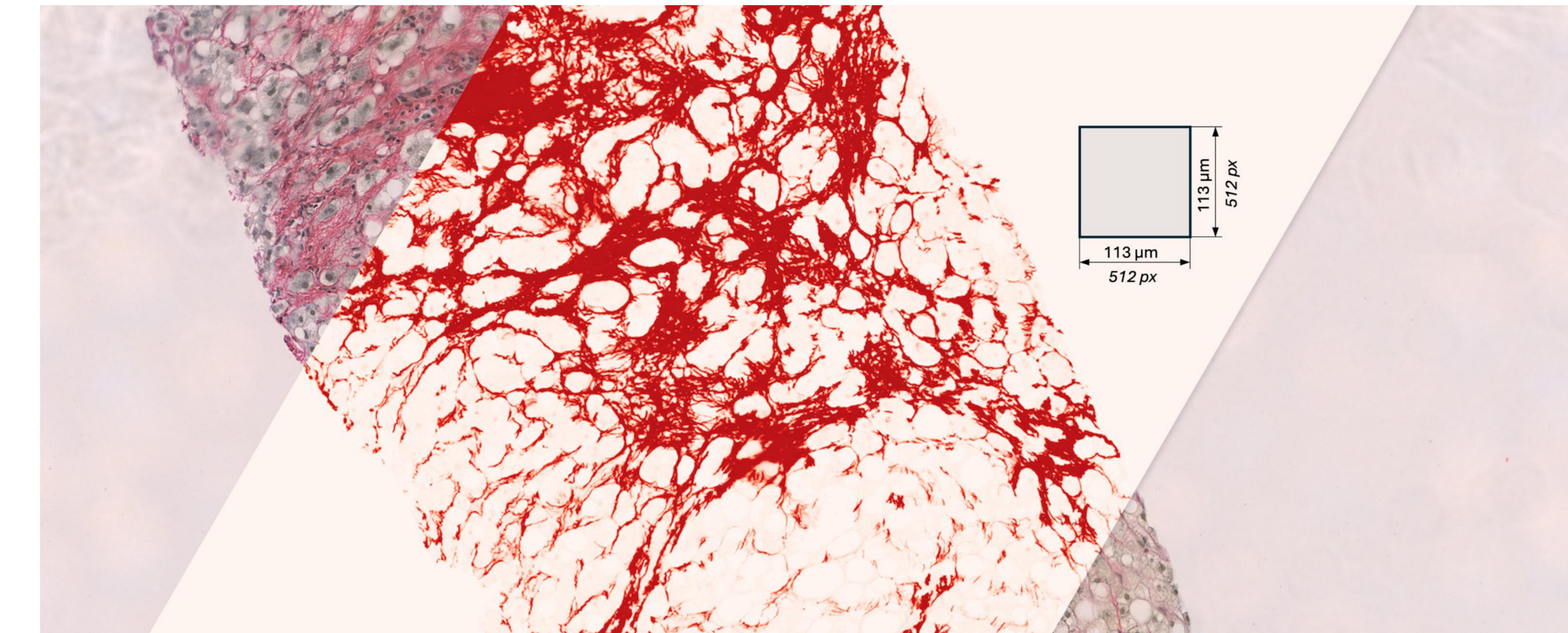
Marta.Wojciechowska@ndm.ox.ac.uk
Mira.Thing@regionh.dk



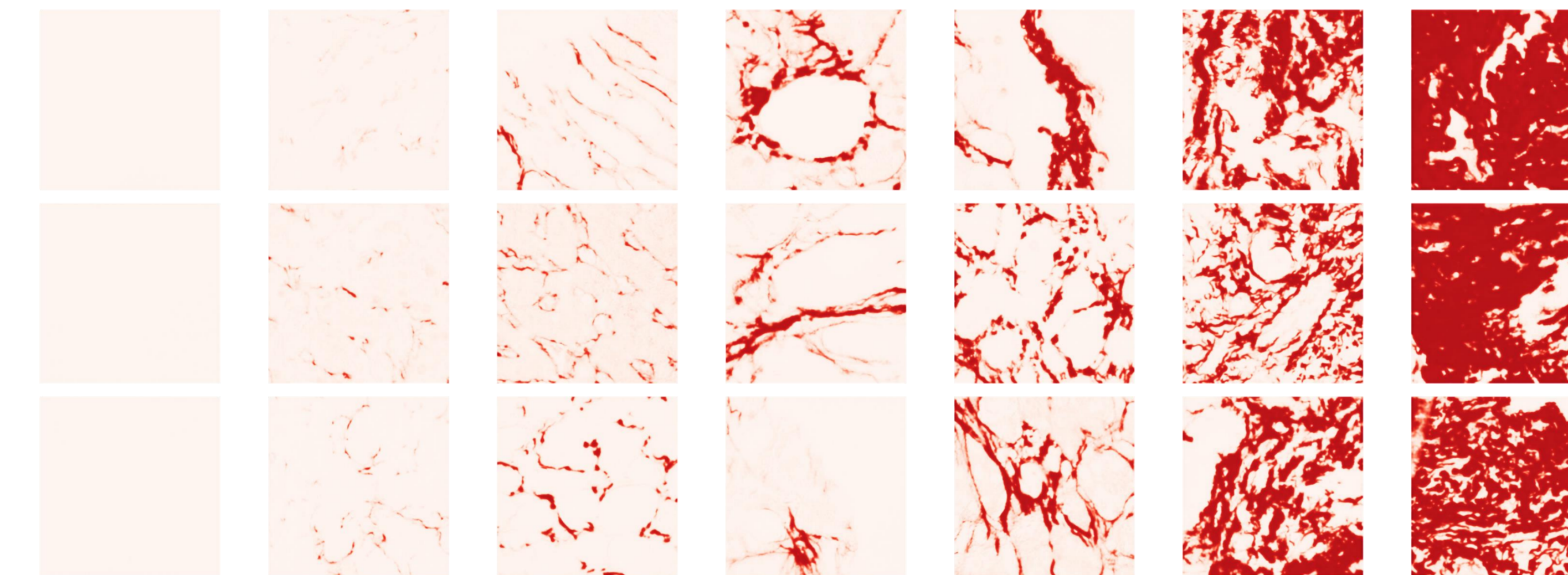
Online version

Methods

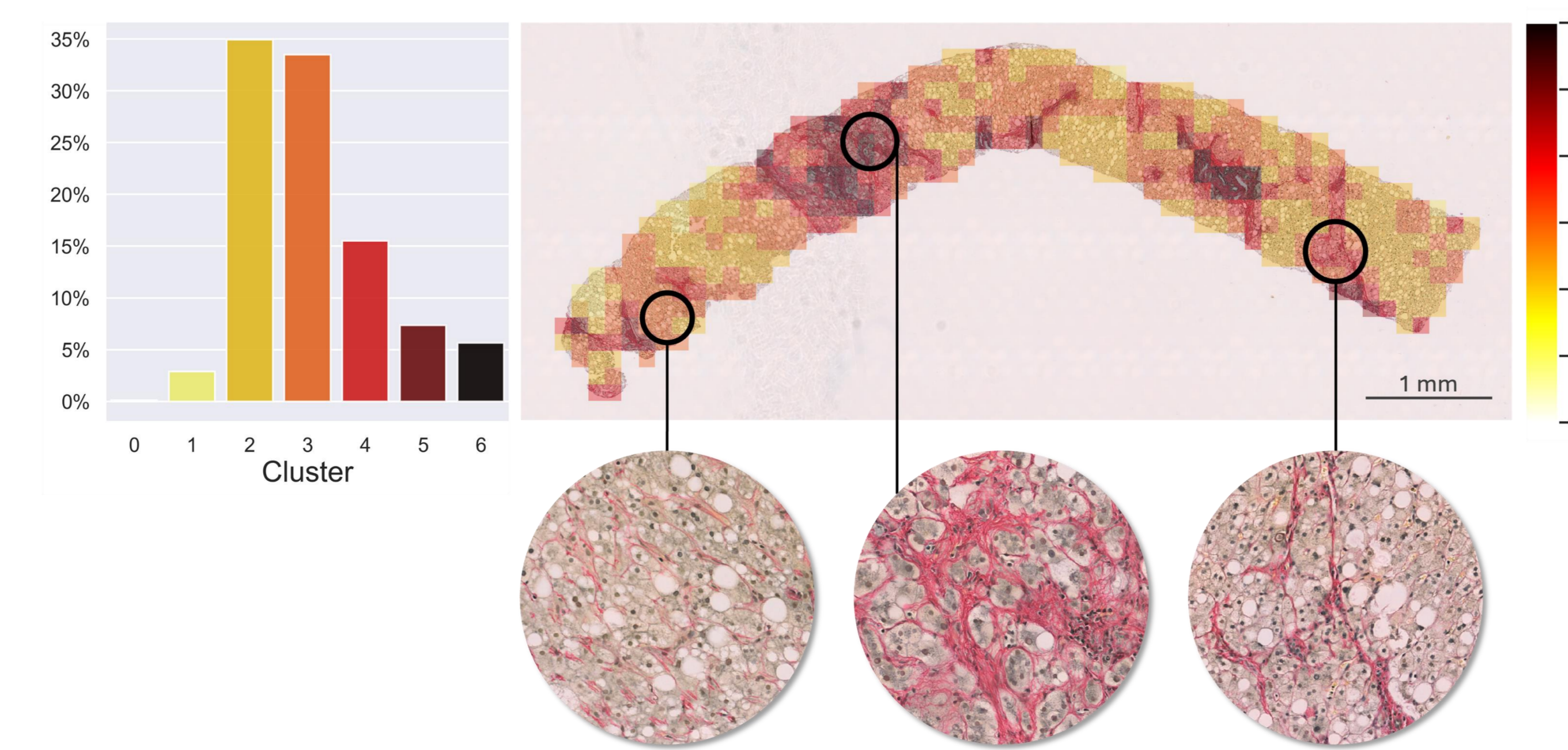
We've developed a novel digital pathology pipeline for collagen analysis.



Collagen fibres are identified from Picrosirius Red (PSR)-stained slides with high precision by a U-net deep learning network.

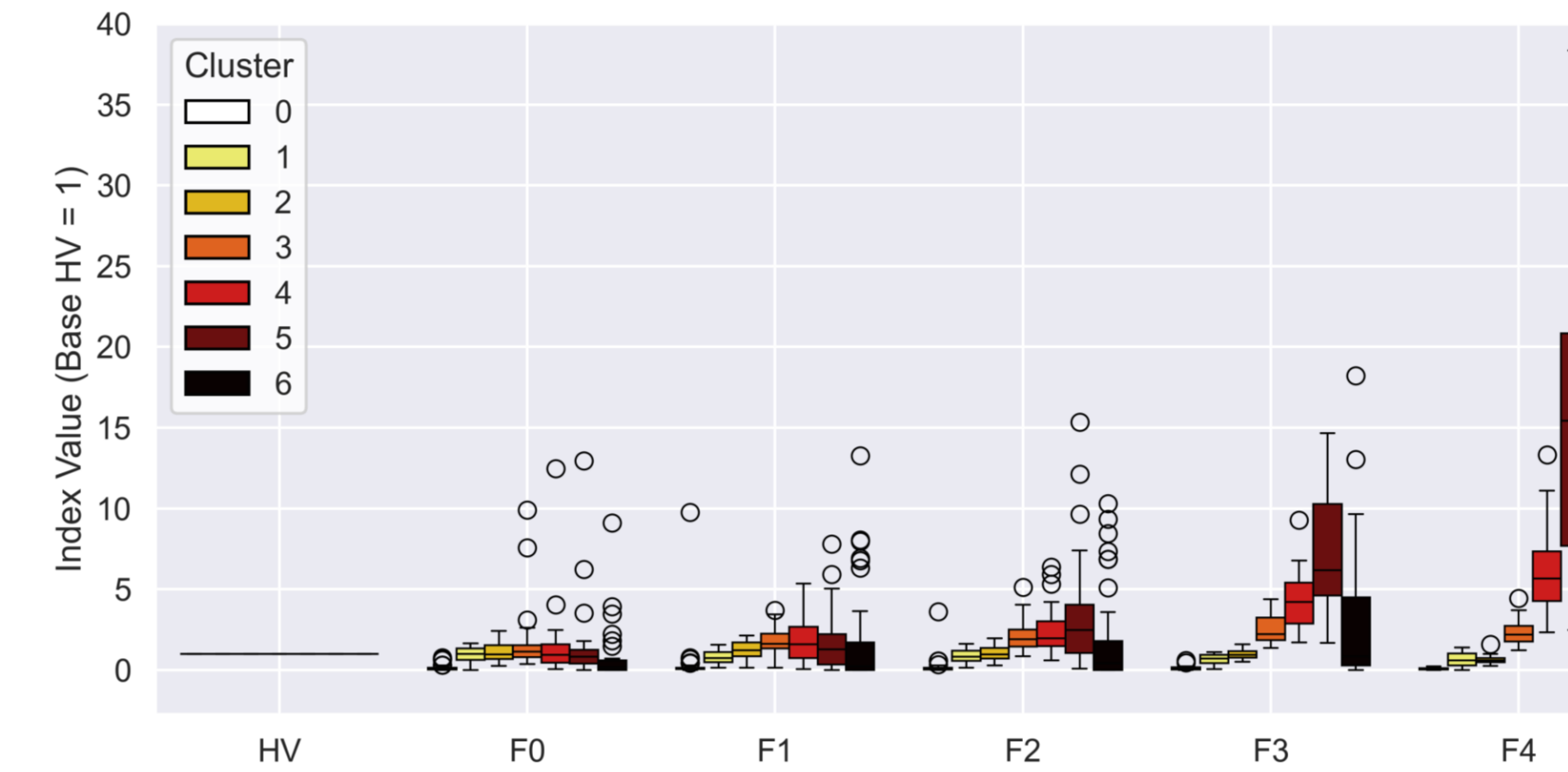


AI was leveraged to identify 7 clusters of ECM patterns, ranging from no identifiable collagen (0), through normal parenchymal ECM (1) to increasingly collagen-dense anatomical and pathological structures (2-5), and scars (6).



The trained AI model for collagen clusters ECM allows to map spatial distribution of fibrosis and to quantify the different components of ECM architecture.

Results

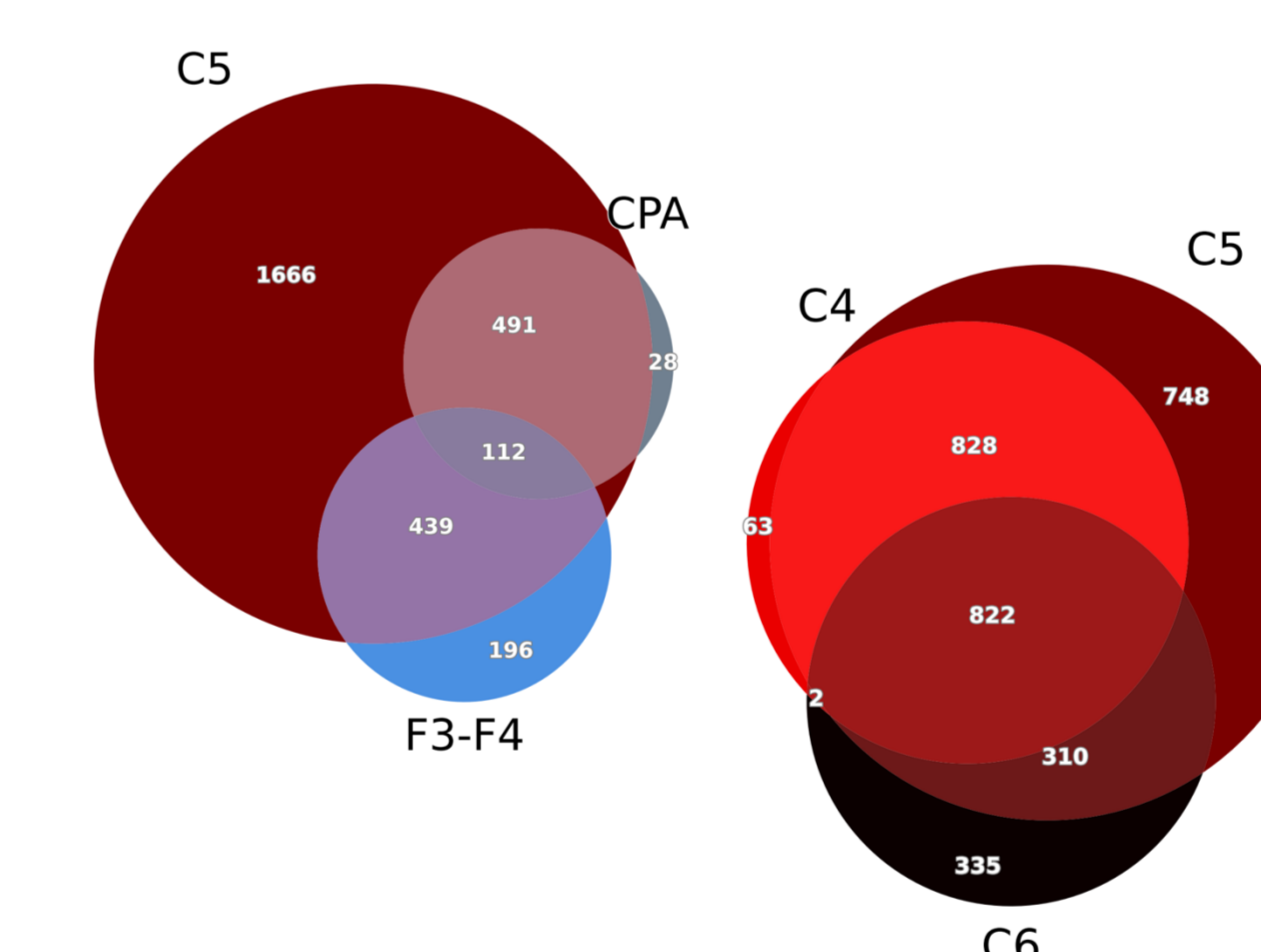


Prediction of clinical outcome

C5 is an independent predictor of liver-related events on par with CPA and fibrosis score.

Further studies are needed to find evidence of improvement in risk stratification.

Number of Common Differentially Expressed Genes

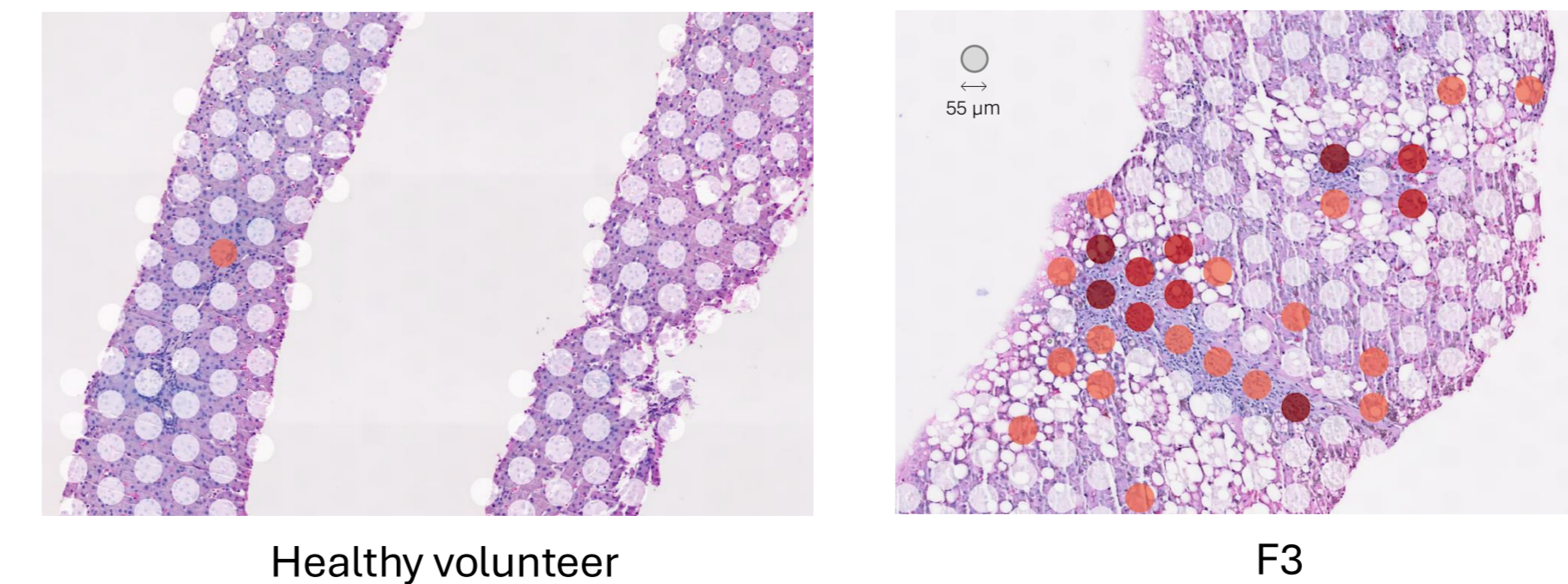


Biological discovery directly from clinical slides

Collagen clusters are strongly associated with known biomarkers of fibrogenesis (e.g. COL10A1) and link them with morphological features of the ECM.

Unlike CPA, collagen clusters offer a fine-grained description of progression and regression of fibrosis.

Local expression of COL10A1 in spatial transcriptomics

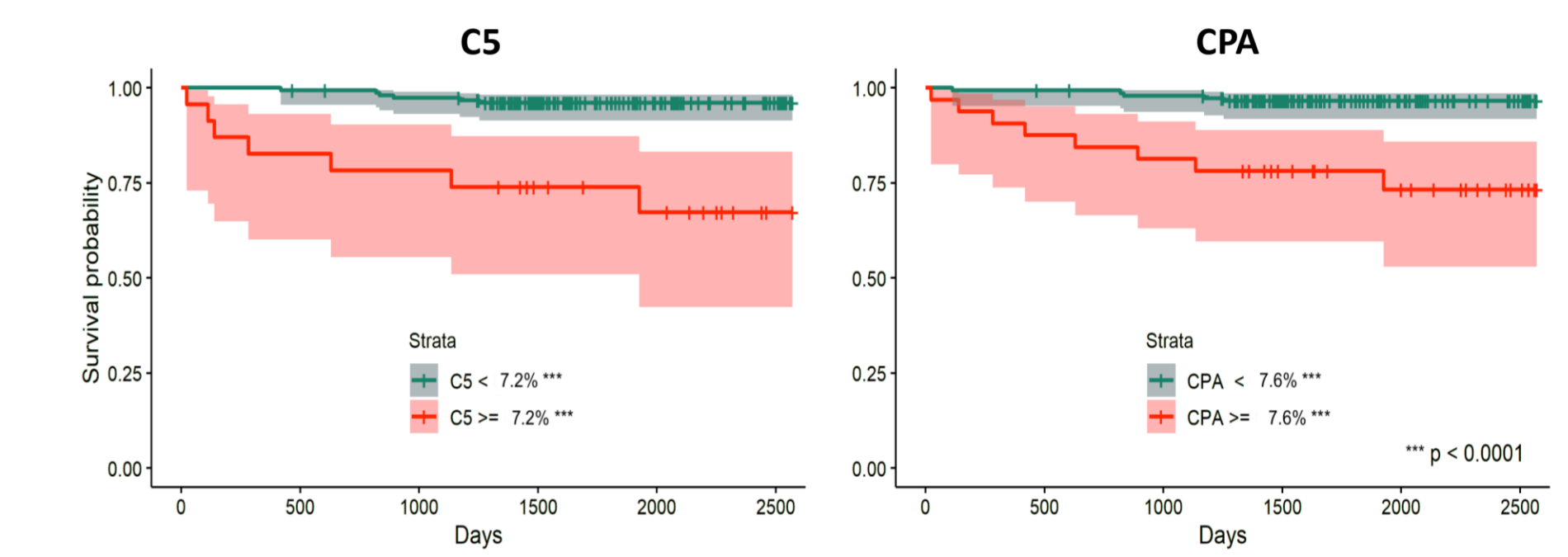


Alignment with fibrosis staging

Collagen clusters disentangle CPA into morphological subtypes of fibrosis.

Tissue proportions of collagen clusters C4, C5 and C6 increase significantly in advanced fibrosis.

Cluster 5 (C5) is the strongest predictor of bridging fibrosis and cirrhosis.



Transcriptomic illumination

Collagen clusters C4-C6 are significantly more sensitive transcriptomic markers of fibrosis than histology score and CPA – allowing to screen for more molecules.

Proportion of C5 is significantly correlated with the highest number of differentially expressed genes, which indicates this cluster identifies areas most actively involved in fibrosis.

Gene	Top Upregulated Genes					Top Downregulated Genes				
	C4	C5	C6	F3-F4	CPA	C4	C5	C6	F3-F4	CPA
STMN2	32	50	28	29	17	novel protein	-24	-21	-27	-22
KRT22	17	30	10	14	16	CALML6	-19	-11	-25	-20
KRT23	3	44	35	14	16	DEFA3	-21	-28	-13	-20
EPHA8	17	30	10	14	16	PRG4	-21	-11	-25	-20
EPH2	17	30	10	14	16	novel protein	-19	-15	-25	-20
EPH3	17	30	10	14	16	novel protein	-19	-15	-25	-20
MUC2B	21	31	29	4	18	MPL3	-19	-15	-25	-20
C2MIP	19	31	31	6	17	GRAP3	-17	-25	-13	-18
CNN1	18	27	35	3	17	COL23	-17	-25	-13	-18
SH2B3	19	31	31	4	17	PINK1	-20	-14	-18	-18
DREP1	23	21	34	11	11	SIGLEC14	-20	-14	-18	-18
BHLHE22	19	25	34	11	15	KRT22	-18	-28	-13	-18
KDRV1-AS2	26	31	34	10	15	DHRS2	-16	-25	-13	-18
FGF7	23	34	34	5	15	CDH4	-16	-24	-13	-18
SMO2	24	31	25	8	15	GPR156	-15	-24	-13	-18
FOLY1	23	31	32	4	16	DEFA19	-15	-24	-13	-18
FAP	21	33	33	8	16	novel protein	-23	-18	-23	-13
GRIN2A	20	31	31	6	16	RTN4	-18	-24	-23	-13
COL18A1	24	25	25	6	16	NRAP	-17	-24	-23	-13
EDL3	23	27	27	6	16	TEC2B	-17	-24	-23	-13
LRMS4	22	31	31	6	16	ZHX1-Cburr76	-17	-24	-23	-13
TYRP1	20	27	27	5	18	PVALB	-14	-24	-11	-17
CHGB	15	25	25	11	17	MTFR1	-14	-24	-11	-17
PCDHAS	18	23	23	3	17	TRIP2-C59K1E	-17	-23	-11	-14
AP0D	16	24	24	4	16	CPNE6	-17	-23	-11	-14
R3HDM1	15	24	24	4	16	CPNE6	-17	-23	-11	-14
SNTO2	12	22	22	3	16	MAJN	-18	-23	-11	-14
SLC6A11	18	21	21	13	16	LOC7242	-18	-23	-11	-14
GPC3	21	21	21	9	15	FAM151A	-14	-21	-11	-14
TRIP4	21	21	21	9	14	PRKDC	-14	-21	-11	-14
TMEM133C	20	21	21	8	15	MAG	-14	-21	-11	-14

The values for C4, C5, C6 and CPA represent change associated with 1% increase in each respective metric. Values for F3-F4 represent fold increase vs. F0-F2. Only values meeting the statistical significance threshold of adjusted P < 0.05 (Bonferroni) are displayed.

Power in numbers

Our modular method can be applied to retrospective studies and large cohorts – supplementing the local precision of spatial transcriptomics.

We are extending this approach to other features of liver disease.

